



Molecular Modelling Studies atom based of 3-Bromo-4-(1-H-3-Indolyl)-2,5-Dihydro-1H-2,5-Pyrroledione Derivatives Antibacterial activity against *Staphylococcus Aureus*

M. C. Sharma^{*a}, Smita Sharma^b, D. V. Kohli^c, S. C. Chaturvedi^d

^a School of Pharmacy, Devi Ahilya Vishwavidyalaya, Indore (M.P), India

^b Department of Chemistry, Yadhunath Mahavidyalaya, Bhind (M.P), India

^c Department of Pharmaceutical Sciences, Dr. Hari Singh Gour University, Sagar (M.P), India

^d Shri Arvindo Institute of Pharmacy, Ujjain Road, Indore (M.P), India

Abstract

A three dimensional quantitative structure-activity relationship study using the atom based 3D QSAR analysis of 3-Bromo-4-(1-H-3-Indolyl)-2,5-Dihydro-1H-2,5-Pyrroledione derivatives had been undertaken with an aim to develop potent antibacterial agent using Schrödinger Software (Maestro8.5) on Linux operating system. The novel Three-Dimensional QSAR (3D-QSAR) study based on the principle of the alignment of pharmacophoric features by PHASE module of Schrodinger suite has been carried out on the same set of inhibitors. Statistically significant 3D ($r^2=0.9057$) QSAR models were generated using 37 molecules in the training set and 12 molecules in the test set.

Key-words -3D QSAR, PHASE, atom based, Antibacterial, *Staphylococcus aureus*.

Introduction

The incidence of infections caused by multidrug-resistant Gram positive bacteria is increasing despite advances in antibacterial therapy over the last decades. As the pathogens causing these infections are frequently resistant to most currently available antibacterials, they are extremely difficult to treat. Almost all bacteria treated with antibiotics have developed at least some degree of resistance against these drugs [1].

The emergence of high levels of penicillin resistance followed by the evolvement and spread of strains resistant to the semisynthetic penicillins (methicillin, and oxacillin), macrolides, tetracyclines, aminoglycosides and glycopeptides (e.g., vancomycin) has made therapy of staphylococcal diseases a global challenge. In many countries, an increasing number of clinical isolates of multi resistant *Staphylococcus aureus* strains have been observed and the

pathogenetic potential in nosocomial and community acquired infections is well known [2]. Efflux pumps compromise the efficacy of a wide range of antibiotics by actively extruding them from bacterial cells [3-4]. The pumps can be expressed in many different forms in both Gram-positive [5] and Gram-negative bacteria, [6] and for some species a variety of pumps may be present with different or overlapping substrates. For the important community and nosocomially acquired human pathogen *Staphylococcus aureus* a number of pumps have been identified, including NorA, which has been shown to play a role in the development of clinical multidrug resistance (MDR) by this organism [7]. One promising strategy for combating MDR in *S. aureus* is to treat infections with a combination of a NorA efflux pump inhibitor and a conventional antibiotic, with the pump inhibitor serving to restore the antibiotic's potency by reducing its efflux from bacterial cells [8]. In the recent past, some efforts have been made to understand three-dimensional quantitative structure–activity relationships, 3D QSAR, on oxazolidinone antibacterial agents using comparative molecular field analysis (CoMFA) [9-13].

Materials and Methods

Data set

The data set consist of structurally diverse compounds reported for antibacterial activity against *S.aureus* 134/93. The selected series of 3-bromo-4-(1H-3-indolyl)-2,5-dihydro-1H-2,5-pyrroledione derivatives having 55 compounds out of which 49 compounds having well defined biological activity reported by Mahboobi. S. et al [14] (Table 1). The antibacterial activity of compounds in the series is reported as pMIC values. The compounds in the selected series were randomly divided in to two sets with 35 compounds used as a training set and the remaining 14 as test set in the prediction of biological activity.

Molecular-Modelling

Three-dimensional structure building, pharmacophore mapping and CoMFA 3DQSAR studies were carried out on a Silicon Graphics Octane (R12000) workstation with the IRIX 6.5 operating system running the SYBYL program package, version 7.2 (Tripos Associates, St. Louis, MO) and the PHASE 1.0 program (Schrödinger Inc., San Diego, CA). Molecular energy minimizations were performed using the Tripos force field with a distance-dependent dielectric constant and the Powell conjugate gradient algorithm with an energy change convergence criterion of 0.001 kcal/mol Å³. Partial atomic charges were calculated using the Gasteiger–Huckel program in SYBYL. All the molecules in the present study were aligned to the best-generated pharmacophore hypothesis (Pharm_A) obtained from the PHASE pharmacophore mapping exercise.

Generation of pharmacophore models

PHASE 1.0 implemented in the Maestro 7.0 modelling package (Schrödinger Inc., San Diego, CA) was used to generate Pharmacophore models for antibacterial activity. The 3D structures of all the molecules used in PHASE were built in, and imported from SYBYL. Conformers of each molecule were generated using the MMFF force field in the PHASE program. Pharmacophore feature sites for the molecules were assigned using a set of features defined in PHASE as hydrogen-bond acceptor (A), hydrogen-bond donor (D), hydrophobic group (H), negatively charged group (N), positively charged group (P), and aromatic ring (R). Three highly active compounds, Common pharmacophore hypotheses were identified using conformational analysis and a tree-based partitioning technique. The resulting pharmacophores were then scored and ranked. Pharmacophores with high-ranking scores were validated by a partial least square (PLS) regression-based PHASE 3D-QSAR cross-

validation, and the best pharmacophore hypothesis identified was further validated by CoMFA 3D-QSAR modelling. All the molecules used for QSAR studies were aligned to the pharmacophore hypothesis obtained in PHASE. The software used for 3-D QSAR study is Schrodinger PHASE Module Workstation used are raster systems in which a computer with Linux as operating systems, 180 giga bite space storage facility Intel Pentium IV as a processor and integrated with graphical display. PHASE module works as a following five steps as: Selection of training set, generating conformers, Find hypothesis for actives, Score hypothesis, Built QSAR model. This 3D-QSAR approach involves the generation of a common pharmacophore hypothesis built on the principle of identification and alignment of pharmacophoric features of the chemical structures. QSAR models are then developed for the pharmacophore hypothesis using the training set structures that match the pharmacophore on three or more sites, using Partial Least Square (PLS) statistical analysis. The volume occluded maps, generated for the pharmacophore hypothesis help in explaining the observed variation in activity by the variation in the structural features.

Computational details for 3D QSAR

In the 3D-QSAR approach, all molecular modeling and statistical analyses were performed using PHASE [15]. PHASE is a versatile product for pharmacophore perception, structural alignment, activity prediction, and 3-D database creation and searching. Given a set of molecules with affinity for a particular target, PHASE utilizes fine-grained conformational sampling and a range of scoring techniques to identify common pharmacophore hypothesis, which convey characteristics of 3-D chemical structures that are purported to be critical for binding. Each hypothesis is accompanied by a set of aligned conformations that suggest the relative manner in which the molecules are likely to bind to the receptor. Generated hypothesis with the aligned conformations may be combined with known activity data to create 3D-QSAR model that identifies overall aspects of molecular structure that govern activity. PHASE 3D-QSAR model workflow consists of the following five steps

I. Preparing ligands

The 3-D conversion and minimization was performed using LigPrep [16] (MMFF force field) incorporated in PHASE. Developing a pharmacophore model requires all-atom 3-D structures that are realistic representations of the experimental molecular structure. Most ligands are flexible, so it is important to consider a range of thermally accessible conformational states in order to increase the chances of finding something close to the putative binding mode. For purpose of pharmacophore model development, PHASE provides two built-in approaches, both of which employ the MacroModel conformational search engine. Conformers were generated using a rapid torsion angle search approach followed by minimization of each generated structure using MMFF force field, with implicit distance dependent dielectric solvent model. A maximum of 100 conformers were generated per structure using a preprocess minimization of 100 steps and post process minimization of 50 steps. Each minimized conformer was filtered through a relative energy window of 11.4 k Cal/mol (50 kJ/mol) and a minimum atom deviation of 2.00 Å.

II. Creating pharmacophore sites

The second step in developing a pharmacophore model is to use a set of pharmacophore features to create sites for all the ligands. Each ligand structure is represented by a set of points in 3-D space, which coincide with various chemical features that may facilitate noncovalent binding between the ligand and its target receptor. PHASE provides a built-in set of six pharmacophore features, hydrogen bond acceptor (A), hydrogen bond donor (D), hydrophobic group (H), negatively ionizable (N), positively ionizable (P), and aromatic ring

(R). The rules that are applied to map the positions of pharmacophore sites are known as feature definitions, and they are represented internally by a set of SMARTS patterns. Each pharmacophore feature is defined by a set of chemical structure patterns. All user-defined patterns are specified as SMARTS queries and assigned one of the three possible geometries, which define physical characteristic of the site:

Point: the site is located on a single atom in the SMARTS query.

Vector: the site is located on a single atom in the SMARTS query, and it will be assigned directionality according to one or more vectors originating from the atom.

Group: the site is located at the centroid of a group of atoms in the SMARTS query. For aromatic rings, the site is assigned directionality defined by a vector that is normal to the plane of the ring. A default setting having acceptor (A), donor (D), hydrophobic (H), negative (N), positive (P), and aromatic ring (R) was used for the creation of pharmacophore sites. No user-defined feature was employed for the present study.

III. Finding a common pharmacophore

In the find common pharmacophore step, pharmacophores from all conformations of the ligand in the active site are examined, and those pharmacophores that contain identical sets of features with very similar spatial arrangements are grouped together. If a given group is found to contain at least one pharmacophore from each ligand, then this group gives rise to a common pharmacophore. Any single pharmacophore in the group ultimately become a common pharmacophore hypothesis which gives an explanation how ligands bind to the receptor. Common pharmacophores are identified using a tree based partitioning technique that groups together similar pharmacophores according to their intersite distances, i.e., the distances between pairs of sites in the pharmacophore. Active and inactive thresholds of PIC₅₀ respectively, were applied to the training set for developing the common pharmacophore hypotheses. After applying default feature definitions to each ligand, common pharmacophores containing six sites were generated using a terminal box size of 1.5 Å, and with requirement that all actives should match.

IV. Scoring Hypotheses

In the score hypotheses step, common pharmacophores are examined, and a scoring procedure is applied to identify the pharmacophore from each surviving n-dimensional box that yields the best alignment of the active set ligands. This pharmacophore provides a hypothesis to explain how the active molecules bind to the receptor. The scoring procedure provides a ranking of the different hypotheses, allowing making rational choices about which hypotheses are most appropriate for further investigation. Scoring with respect to actives was conducted using default parameters for site, vector, and volume terms. Ligand activity, expressed as -log₁₀ (IC₅₀), was incorporated into the score with a weight of 1.0, and relative conformational energy (kJ/mol) was included with a weight of 0.01. Hypotheses that emerged from this process were subsequently scored with respect to inactive, using a weight of 1.0. The inactive molecules were scored to observe the alignment of these molecules with respect to the pharmacophore hypothesis to enable making a decision on the selection of the hypothesis. Larger is the difference between the scores of active and inactive, better is the hypothesis at distinguishing the actives from inactive.

V. Building QSAR model

PHASE provides the means to build QSAR models using the activities of the ligands that match a given hypothesis. PHASE QSAR models are based on PLS regression, applied to a large set of binary valued variables. The independent variables in the QSAR model are

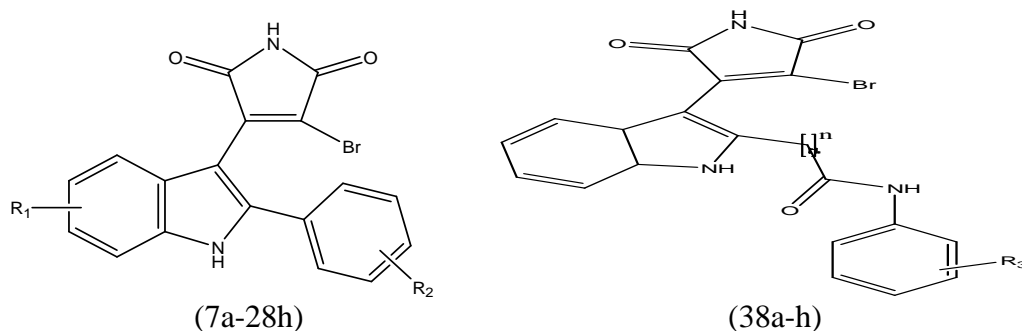
derived from a regular grid of cubic volume elements that span the space occupied by the training set ligands. Each ligand is represented by a set of bit values (0 or 1) that indicate which volume elements are occupied by a Vander Waals surface model of the ligand. To distinguish different atom types that occupy the same region of space, a given cube in the grid may be allocated as many as six bits, accounting for six different classes of atoms. The atoms classes are: D: hydrogen-bond donor, H: hydrophobic or nonpolar, N: negative ionic, positive ionic, electron-withdrawing (includes hydrogen-bond acceptors), miscellaneous (all other types). PHASE QSAR models may be either atom-based or pharmacophore-based, the difference being whether all atoms are taken into account, or merely the pharmacophore sites that can be matched to the hypothesis. The choice of which type of model to create depends largely on whether or not the training set molecules are sufficiently rigid and congeneric. If the structures contain a relatively small number of rotatable bonds and some common structural framework, then an atom-based model may work quite well. Atom-based QSAR models were generated for AHRRRR hypothesis using the 55-member training set and a grid spacing of 1.0Å. QSAR models containing one to seven PLS factors were generated. A model with five PLS factors was considered as the best statistical model. This model was validated by predicting activities of test set molecules.

Analysis of Atom-Based PHASE Model

Figure 5, 6, 7 shows the volume occlusion maps for the atom-based PHASE 3D-QSAR model (donor, hydrophobic, and electronegative) represented by color codes. These maps represent the regions of favourable and unfavourable interactions. The volume occlusion maps of hydrogen bond donor (Figure.5) describe the spatial arrangement of favourable hydrogen bonding interactions to acceptor groups of the target protein. In figure-5, 6, 7 red regions indicates unfavourable region for substitution and blue region indicates favourable region for substitution.

Result and Discussion

In 3D-QSAR analysis of 3-Bromo-4-(1-H-3-Indolyl)-2,5-Dihydro-1H-2,5-Pyrroledione derivatives it was found that Correlation Coefficient (r^2) = 0.9057, Cross validation Coefficient (q^2)=0.0207, & Standard Deviation(S.D)=0.211 (Table3). From fig 5, 6, 7 it was found that on substituting hydrogen bond donor or electron withdrawing group or hydrophobic group to compounds (34a-h) having a substituted anilide substructure linked to the indole-2 position by alkyl spacer shall increase antibacterial activity, on substituting electron withdrawing group at 5-position of indole shall decrease activity, on substituting hydrophobic group at 5 & 7 position of indole shall increase antibacterial activity. Where, Aromatic Ring (R) Orange torus in the plane of the ring, Acceptor (A) Light red sphere centered on the atom with the lone pair, with arrows pointing in the direction of the lone pairs, Donor (D) Light blue sphere centered on the H atom, with an arrow pointing in the direction of the potential H-bond, Hydrophobic (H) Green sphere.

Table 1: Activity of 3- bromo-4-(1-H-3-indolyl)-2, 5-dihydro-1H-2, 5-Pyrroledione derivatives against Staphylococcus aureus 134/93

Nr	R1	R2	MIC*10 ⁻⁶	pMIC
7a	H	4-OMe	0.32	6.5
7b	H	4-OBu	0.45	6.3
7c	H	4-OPen -	0.88	6.1
7d	H	4-Oct	50	4.3
7f	H	4-OBzl	0.21	6.7
7g	H	4-ONaph	1.5	5.8
12a	5-OMe	H	1.00	6.0
12b	5-OEt	H	3.80	5.4
12c	5-OPr	H	0.95	6.0
12d	5-OBu	H	0.11	6.9
12e	5-Open	H	27	4.6
13a	5-OEt	4-OMe	2.0	5.7
13b	5-OPr	4-OMe	0.44	6.4
13c	5-OBu	4-OMe	0.10	7.0
18a	5-OMe	H	0.13	6.9
18b	5-Et	H	0.13	6.9
18c	5-Pr	H	0.50	6.3
18d	5-Bu	H	0.24	6.6
18e	5-Pen	H	0.91	6.0
19a	5-Me	4-OMe	0.12	6.9
19b	5-Et	4-OMe	0.23	6.6
19c	5-Pr	4-OMe	0.45	6.3
19d	5-Bu	4-OMe	0.44	6.4
19e	5-Pen	4-OMe	0.85	6.1
24a	7-Me	H	3.98	5.4
24b	7-Et	H	2.51	5.7
24c	7-Bu	H	0.25	6.6
24d	7-Pen	H	0.50	6.3
25a	7- Me	4-OMe	2.00	5.7

25b	7- Et	4-OMe	0.50	6.3
25c	7- Pr	4-OMe	0.50	6.3
25d	7- Bu	4-OMe	0.25	6.6
25e	7- Hex	4-OMe	0.40	6.4
28a	5-OMe	3- OMe	1.90	5.7
28b	5-OEt	3- OMe	3.50	5.5
28c	5-OBu	3- OMe	3.30	5.5
28d	5-OMe	3- OMe	12.60	4.9
28e	5-Me	3- OMe	0.20	6.6
28f	5-Et	3- OMe	0.50	6.3
28g	5-Bu	3- OMe	3.40	5.5
28h	5-Hex	3- OMe	26.00	4.6
34a	2	H	0.18	6.7
34b	3	H	1.7	5.8
34c	4	H	1.7	5.8
34d	5	H	0.10	7.0
34e	6	H	0.10	7.0
34f	3	4-Me	1.58	5.8
34g	3	3-Me	0.79	6.1
34h	3	2-Me	0.32	6.5
ciprofloxacin			38.1	4.4

MIC* indicates Minimum Inhibitory Concentration

Table 2: Fitness and activity

Ligand Name	QSAR Set	Activity	PLS Factor	Predicted Activity	Pharm Set	Fitness
7a	training	6.49	4	6.35		2.87
7b	training	6.34	4	6.27		2.77
7c	test	6.05	4	6.09		2.75
7d	test	4.30	4	6.35	inactive	2.67
7f	training	6.67	4	6.67	active	2.71
7g	training	5.82	4	5.92		2.67
12a	training	6	4	6.27		2.95
12b	test	5.42	4	6.07	inactive	2.89
12c	training	6.02	4	6.2		2.88
12d	training	6.95	4	6.52	active	2.84
12e	training	4.56	4	4.39	inactive	2.81
13a	test	5.69	4	6.25	inactive	2.82
13b	training	6.35	4	6.4		2.82
13c	training	7	4	6.71	active	2.78
18a	training	6.88	4	6.59	active	3
18b	test	6.88	4	6.65	active	2.95
18c	training	6.30	4	6.59		2.92
18d	training	6.62	4	6.39	active	2.88
18e	test	6.04	4	6.18		2.84
19a	test	6.92	4	6.77	active	2.92

19b	training	6.63	4	6.76	active	2.88
19c	test	6.34	4	6.69		2.85
19d	training	6.35	4	6.5		2.81
19e	training	6.07	4	6.28		2.78
24a	training	5.4	4	5.68	inactive	2.9
24b	training	5.6	4	5.75	inactive	2.86
24c	test	6.60	4	6.32	active	2.8
24d	training	6.30	4	6.43		2.77
25a	training	5.69	4	5.88	inactive	2.83
25b	test	6.30	4	5.93		2.8
25c	training	6.30	4	6.18		2.77
25d	training	6.60	4	6.48	active	2.75
25e	training	6.39	4	5.7		2.69
28a	training	5.72	4	5.7	inactive	2.88
28b	training	5.45	4	5.52	inactive	2.83
28c	training	5.48	4	5.88	inactive	2.78
28d	training	4.9	4	6.48	inactive	2.73
28e	test	6.69	4	5.95	active	2.91
28f	training	6.30	4	6.07		2.88
28g	test	5.46	4	5.98	inactive	2.81
28h	training	4.58	4	4.37	inactive	2.76
34a	training	6.74	4	6.73	active	2.52
34b	training	5.77	4	5.79	inactive	2.6
34c	training	5.77	4	5.55	inactive	2.61
34d	training	7	4	6.88	active	2.54
34e	training	7	4	6.95	active	2.55
34f	test	5.80	4	5.93		2.58
34g	training	6.10	4	5.99		2.58
34h	test	6.49	4	6.07		2.59

Table 3: 3D QSAR Result

ID	PLS Factors	SD	R ²	F	P	RMSE	Q-squared	Pearson-R
ADHRR.86	4	0.211	0.9057	72	6.05e-15	0.6745	0.0207	0.2949

Table.4 QSAR Hypothesis Score

ID	Survival	Survival – inactive	Post-hoc	Site	Vector	Volume
ADHRR 43	2.145	1.034	2.341	0.98	0.67	0.341
ADHRRR.52	2.790	2.371	3.043	0.98	0.45	0.341
ADRRRR.68	3.142	3.782	3.936	0.98	0.56	0.315
ADRRRR.82	3.537	3.867	4.231	0.93	0.71	0.662
ADRRRR.88	3.781	4.162	4.683	0.92	0.94	0.501
ADHRRR.249	4.449	4.357	4.283	0.92	0.91	0.736
ADHRRR.432	4.901	4.631	4.783	0.94	0.97	0.289

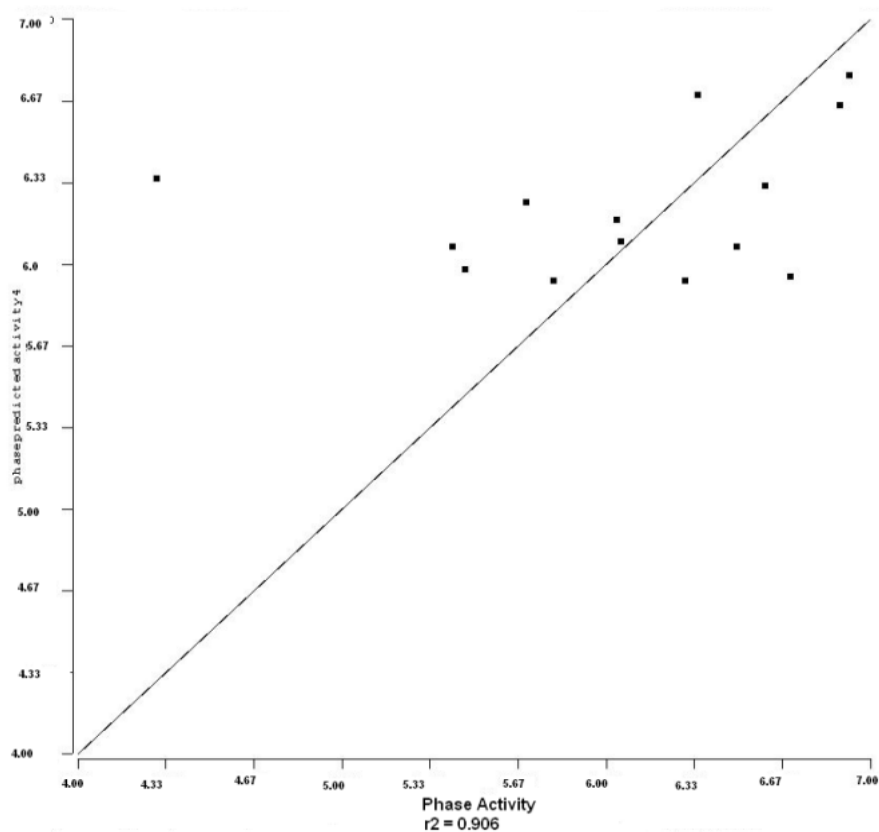
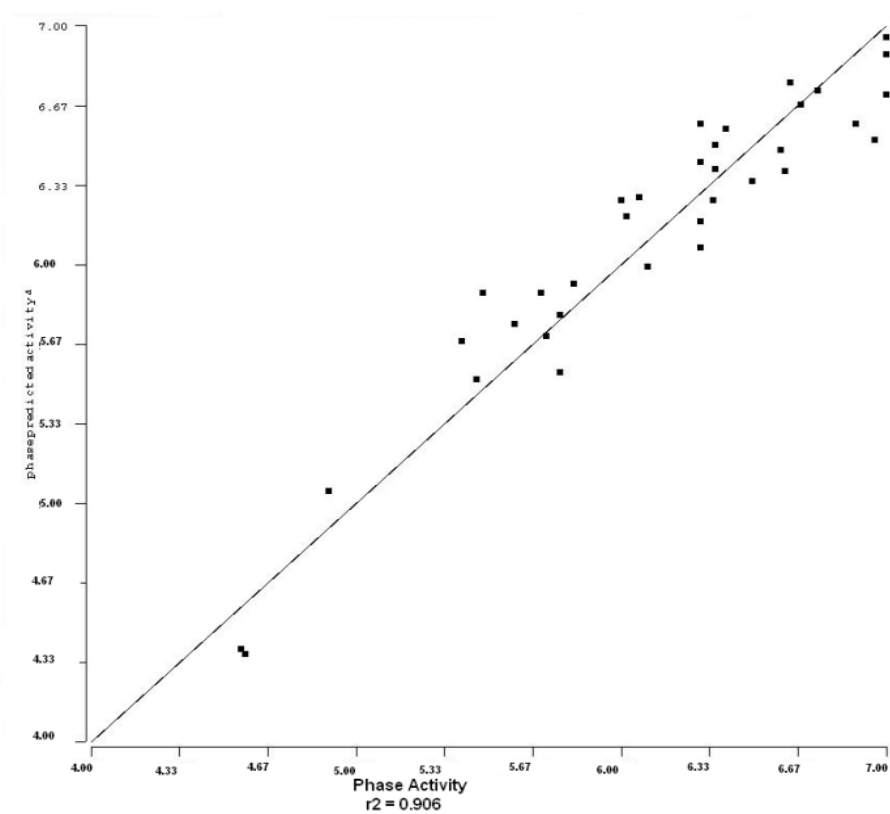
Figure 1: Plot of predicted activity Vs phase activity for test compounds**Figure 2: Plot of predicted activity Vs phase activity for training compounds**

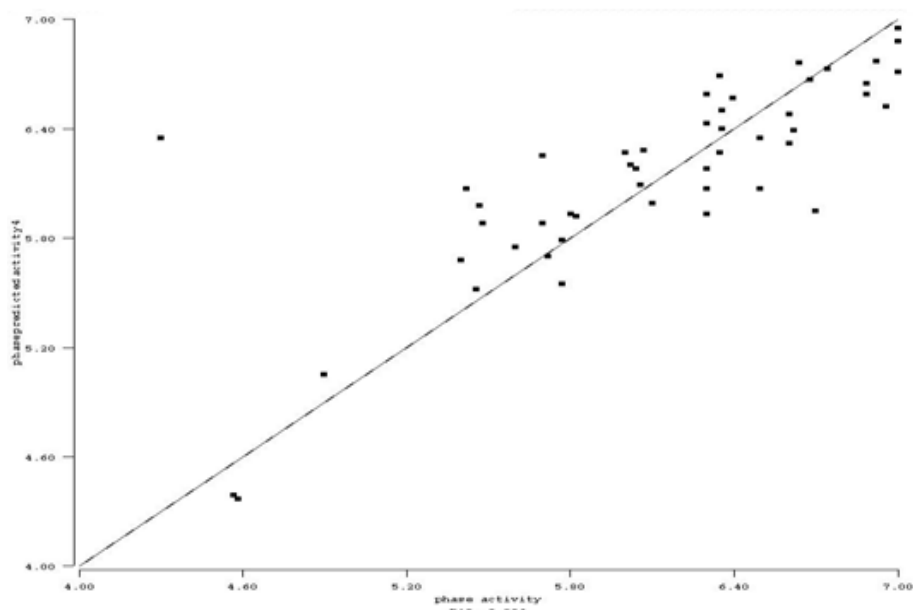
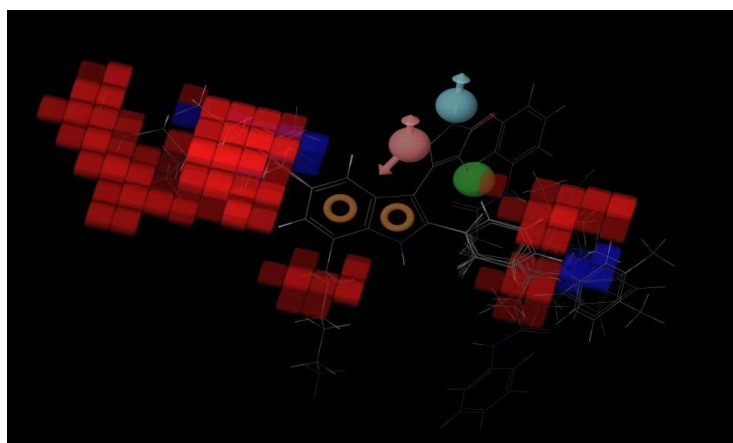
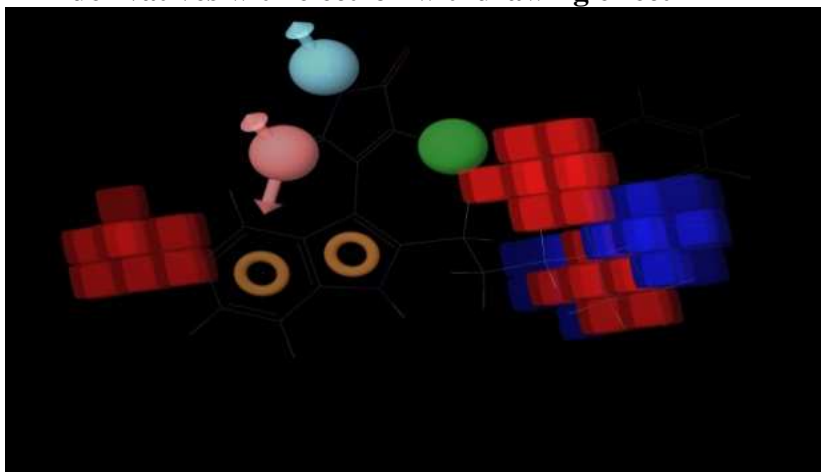
Figure 3: Plot of predicted activity Vs phase activity for all compounds**Fig 4: QSAR Model of 3-Bromo-4-(1-H-3-Indolyl)-2, 5-Dihydro-1H-2,5 Pyrroledione derivatives along with alignment of structures****Fig 5: QSAR Model of 3-Bromo-4-(1-H-3-Indolyl)-2, 5-Dihydro-1H-2, 5-Pyrroledione derivatives with electron withdrawing effect**

Figure 6: QSAR Model of 3-Bromo-4-(1-H-3-Indolyl)-2, 5-Dihydro-1H-2, 5-Pyrroledione derivatives with H-bond donor effect

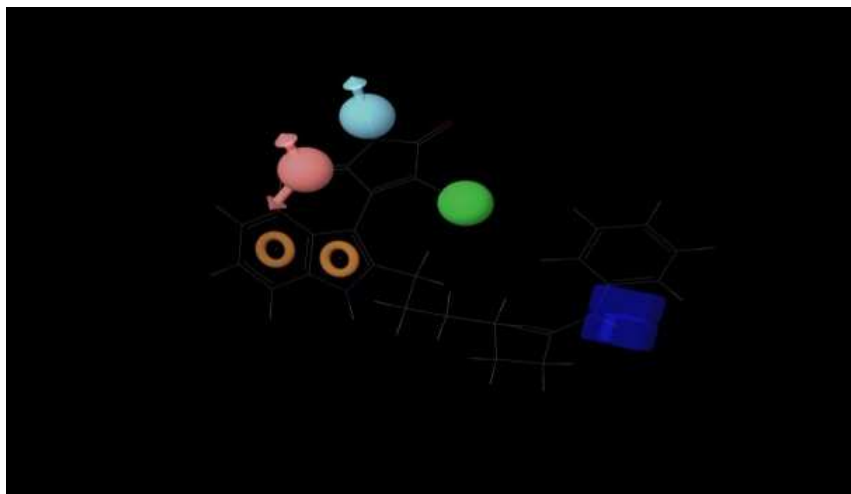
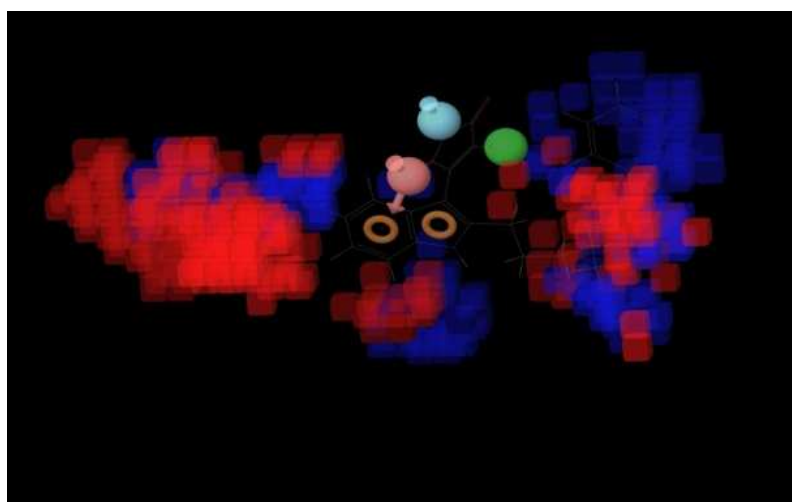


Figure 7: QSAR Model of 3-Bromo-4-(1-H-3-Indolyl)-2, 5-Dihydro-1H-2, 5-Pyrroledione derivatives with hydrophobic effect



Conclusion

A set of 49 compounds of 3-Bromo-4-(1-H-3-Indolyl)-2,5-Dihydro-1H-2,5-Pyrroledione derivatives was subjected to 3D-QSAR analysis using Partial Least Square (PLS) method to design its derivatives as potent antibacterial agent. In fig 4,5,6,7 red regions indicates unfavourable region for substitution, and blue region indicates favourable region for substitution which draws the conclusion that by substituting group at direction identified at QSAR model potent antibacterial agent can be produced.

Reference

- [1] Baquero F., J. *Antimicrob. Chemother.*, **1997**, 39, 1-6.
- [2] Tenover F.C., Biddle J.W., Lancaster M.V., *Emerg. Infec. Dis*, **2001**., 7327-332.
- [3] Marquez B., *Biochimie.*, **2005**, 87, 1137.
- [4] Lomovskaya O., Zgurskaya I.H., Totrov M., Watkins M., *Nat. Rev. Drug. Discov.*, **2007**, 6, 56.

-
- [5] Kaatz G.W., White D.G., Alekshun M.N., McDermott P.F., SM Press, D C Washington, 2005, pp.275.
- [6] Poole K., *Clin. Microbiol. Infect.*, **2004**, 10, 12.
- [7] Kaatz G.W., Seo S.M., Ruble C.A., *Antimicrob. Agents Chemother*, **1993**, 37, 1086.
- [8] Bremner J.B., *Pure Appl. Chem.* **2007**, 79, 2143.
- [9] Pae A.N., Kim S.Y., Kim H.Y., Joo H.J., Cho Y., Choi K.I., Choi J.H., Koh H.Y., *Bioorg. Med. Chem. Lett.*, **1999**, 9, 2685.
- [10] Karki R.G., Kulkarni V.M., *Bioorg. Med. Chem.*, **2001**, 9, 3153.
- [11] Gopalakrishnan B., Khandelwal A., Rajjak S.A., Selvakumar Das N., Trehan S., J Iqbal ., S Kumar. *Bioorg. Med. Chem*, **2003**, 11, 2569.
- [12] AR Katritzky; DC Fara; M Karelson. *Bioorg. Med. Chem*, **2004**, 12, 3027.
- [13] Tokuyama R., Takahashi Y., Tomita Y., subouchi M.T., T Yoshida., N Iwasaki., N Kado., E Okezaki., Nagata O., *Chem. Pharm. Bull.*, **2001**, 49, 353.
- [14] Mahboobi S., Eichhorn E., Winkler M., Sellemer A., Mollmann U., *Eur. J. of Medi. Chem.*, **2008**, 43, 633-656.
- [15] PHASE 2.0, Schrödinger, LLC, New York., NY, **2006**.
- [16] Ligprep 2.0, Schrödinger, LLC, New York., NY, **2006**.